Computational Screening of Perovskite Metal Oxides for Optimal Solar Light Capture† - Electronic Supplementary Information

Ivano E. Castelli,[a] Thomas Olsen,[a] Soumendu Datta,[a] David D. Landis,[a] Søren Dahl,[b] Kristian S. Thygesen,[a] and Karsten W. Jacobsen,*[a]

Received 20th September 2011, Accepted 17th November 2011
First published on the web Xth XXXXXXXXXX 200X
DOI: 10.1039/C1EE02717D

Methods

All calculations are performed for the primitive unit cell containing 5 atoms: 3 oxygen and 2 metals. Each simulation is composed of two part: the optimization of the structure and the calculation of the bandgap.

With respect to the stability, Calle-Vallejo *et al.*[1] have recently shown that the trends in the heat of formation for oxides in the perovskite structure are well reproduced with Density Functional Theory (DFT)[2] using the generalized-gradient-approximation (GGA) in form of the RPBE-functional[3] for the exchange-correlation energy. Even the absolute values of the heats of formation can be determined within a few tenths of an electronvolt per metal atom.[1] We have therefore adopted this scheme for the calculation of stabilities.

For each combination, we scan for the optimal lattice parameter, relax positions of the atoms inside the cell, until the residual forces are less than 0.05 eV $Å^{-1}$ and scan again for the lattice parameter with a mesh of 64 k-points in the Brillouin zone and a grid spacing equal to 0.17. For the total energy calculation,we use a mesh of 216 k-points in the Brillouin zone and a grid spacing equal to 0.15. The calculations performed are converged with respect to these parameters.

The GLLB-SC functional works by adding the derivative discontinuity to the Kohn-Sham gap to obtain the quasi-particle gap. For light harvesting one is really interested in the photo-absorption gap which may differ from the quasi-particle gap because of excitonic effects. However, for the class of materials that we study here we expect these effects to be only moderate. Using this functional, we need a mesh of about 400 k-points. We calculate the GLLB-SC gap only for the combinations with a RPBE direct gap larger than 0.2 eV. This does not affect the screening since we are looking for a material with a visible-light bandgap.

All the calculations are performed on our linux cluster Niflheim with 5640 CPU cores.

A linear programming algorithm (LP) was adopted to determine the stability relative to a pool of reference systems. For the oxides, we include the single-metal bulk and the most stable single-metal oxides and compare them with the DFT energy of the combination in the perovskite structure. We consider a compound non-stable when the ABO_3 energy is 0.2 eV/atom greater than the best outcome from the LP:

$$\begin{aligned} \Delta E &= ABO_3(s) + \\ &- \min_{c_i}(c_1 A\,(s) + c_2 B\,(s) + \\ &+ c_3 A_x O_y\,(s) + c_4 B_x O_y\,(s) + c_5 O)\;, \end{aligned} \tag{1}$$

where A and B are the bulk metals, A_xO_y and B_xO_y are the single metal oxides included in the references and O is simply obtained from $H_2O - H_2$. The problem is solved with the constraints:

$$c_1 + c_3 = 1\;, \qquad c_2 + c_4 = 1\;, \qquad c_3 + c_4 + c_5 = 3\;, \tag{2}$$

for the A, B metals and oxygen, respectively, to obtain the perovskite stoichiometry. A similar analysis has been performed for the oxynitrides with the most stable single- and bi-metal nitrides and single-metal oxynitrides in the pool of reference system and with the constraints that the sum of the oxygen and nitrogen atoms must be equal to 2 and 1, respectively.

Bandgaps of Single-Metal Oxides

In † Table 1 we report the comparison between the theoretical gaps evaluated using the GLLB-SC functional[26,27] with the experimental values in the most stable single-metal oxide structure obtained from the ICSD database.[28] Those values have been used for Fig. 1 in the manuscript. For each structure, we use the same procedure used for the screening: i.e. starting from the experimental data, we find the lattice parameters and we completely relax the internal degrees of freedom using an RPBE functional[3] and afterward we evaluate the gaps using the GLLB-SC functional.

Cubic Perovskite Oxides

† Table 2 reports the combinations that fulfill the conditions for stability and for the gap. We specify the heat of formation and the indirect (direct) bandgap. The heat of formation

Electronic Supplementary Material (ESI) for Energy & Environmental Science

Oxide	GLLB-SC Gap [eV]	Expt. Gap [eV]	Method	Oxide	GLLB-SC Gap [eV]	Expt. Gap [eV]	Method
BeO	10.9	10.6	Optical [4]	Rh_2O_3	1.4	1.2	[5]
MgO	8.1	7.9	Thermal [6]	PdO	0.2	1.0	[7]
CaO	7.7	7.8	Thermal [8]	PtO_2	1.4	1.8	[9]
SrO	7.4	6.4	Thermal [8]	Cu_2O	1.1	2.2	[10]
BaO	5.0	4.4	Thermal [8]	Ag_2O	0.4	1.2	[11]
Sc_2O_3	7.0	6.3	[12]	ZnO	3.3	3.3	Optical [13]
TiO_2 (r)	3.8	3.0	[14]	CdO	1.7	2.2	Optical [15]
TiO_2 (a)	4.6	3.2	[16]	Al_2O_3	9.7	8.8	Optical [17]
ZrO_2 (r)	7.1	6.6	[18]	Ga_2O_3	5.0	4.8	[19]
ZrO_2 (m)	6.8	5.3	[20]	In_2O_3	3.0	2.6	[21]
Nb_2O_5	3.4	3.4	[7]	SnO_2	3.6	3.6	Photoemission [22]
MoO_3	3.2	3.0	[7]	PbO	4.1	2.8	Indirect [23]
WO_3	2.9	2.7	Optical [24]	Bi_2O_3	4.4	2.9	Optical [25]

Table 1 bandgaps: theoretical and experimental bandgap evaluated for the metal oxides included in Fig. 1 of the manuscript. The type of the experimental gap is reported, when available, in the method column.

	ΔE [eV/atom]	Gap [eV]	Band Edges
$TlTaO_3$	0.10	2.0 (2.0)	
$GaTaO_3$	−0.03	2.1 (2.2)	
$SnTiO_3$	0.10	2.5 (2.7)	✓
$CsNbO_3$	0.18	2.8 (2.9)	✓
$AgNbO_3$ [a]	0.20	2.9 (3.5)	✓
$NaVO_3$	0.10	1.0 (1.7)	
$LiVO_3$	0.17	1.3 (2.0)	✓
$BaSnO_3$ [a]	−0.08	2.5	✓
$SrSnO_3$ [b]	0.01	2.9 (3.4)	✓
$CaSnO_3$ [b]	0.16	3.0 (3.6)	✓
$SrGeO_3$	0.16	1.2 (1.7)	✓
$CaGeO_3$	0.16	2.1 (2.7)	✓
$NaSbO_3$	0.20	1.5 (2.6)	✓

Table 2 Cubic Perovskite Oxides: Formation energies (ΔE) per atom and indirect (direct) bandgap for the candidates for a new solar light capture material. It is also indicated (✓) if the band edges match with the water redox potential. [a] The experimental bandgaps for the two known cubic perovskite materials, $AgNbO_3$ and $BaSnO_3$, are equal to 2.8 eV[29] and 3.1 eV[30], respectively. [b] $SrSnO_3$ and $CaSnO_3$ suffer from a lattice distortion and they show an orthorhombic perovskite with a DFT (experimental) bandgaps equal to 4.2 (4.1) eV[30] and 3.8 (4.4) eV[30], respectively.

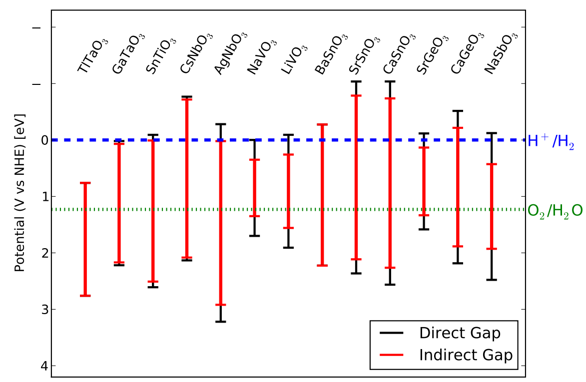

Fig. 1 Band edge position evaluated for the combinations of † Table 2. In the figure, we indicate the band edge position for the indirect (in red) and direct (in black) gap.

is obtained using the linear programming approach with the single-metal bulks, the single- and bi-metal oxides as pool of references. We report also if the band edges match with the water redox potential and the experimental bandgap for the combinations showing a perovskite or a perovskite-like experimental structure.

† Fig 1 reports the band edge positions, evaluated using the empirical rule provided by Butler and Ginley[31] and using the DFT gaps calculated here, for all the combinations of † Table 2. Three combinations do not match with the H^+/H^2 po-

	ΔE [eV/atom]	DFT Gap [eV]	Band Edges	Experimental Gap [eV]
$BaTaO_2N$	−0.01	2.0	✓	2.0 [32]
$SrTaO_2N$	0.00	2.1	✓	2.1 [32]
$CaTaO_2N$	0.09	2.2	✓	2.5 [32]
$MgTaO_2N$	0.19	2.1 (2.8)	✓	
$PbTaO_2N$	0.19	1.9 (2.1)		
$LaTiO_2N$	0.05	2.5	✓	2.1 [33]

Table 3 Cubic perovskite oxynitrides: Formation energies (ΔE) per atom and indirect (direct) bandgap for the candidates for a new solar light capture material. It is also indicated (✓) if the position of the band edges matches with the water redox potential and the experimental bandgap for the cubic perovskites known structures.

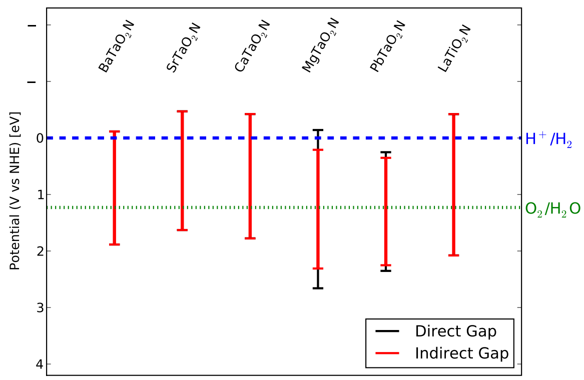

Fig. 2 Band edge position evaluated for the oxynitride combinations of † Table 3.

tential. All the combinations are suitable for oxygen evolution: this is a feature of the oxides.

Including the criteria on the band edge positions in addition to the rules on the heat of formation and on the gaps, we reduce the list of candidates from 13 to the 10 of Fig. 4 in the paper.

Cubic Perovskite Oxynitrides

As in † Table 2 for the oxides, in † Table 3 we list the combinations that comes out after the screening on the stability and on the bandgap. In addition we report if the position of band edges matches with the water redox potential. The experimental values for the gaps are in a good agreement with the DFT values.

† Fig 2 shows the bands position of all the combinations of † Table 3.

References

1 F. Calle-Vallejo, J. I. Martínez, J. M. García-Lastra, M. Mogensen and J. Rossmeisl, *Angewandte Chemie (International ed in English)*, 2010, **49**, 7699–7701.
2 P. Hohenberg and W. Kohn, *Physical Review*, 1964, **136**, 864.
3 B. Hammer, L. B. Hansen and J. K. Nørskov, *Physical Review B (Condensed Matter and Materials Physics)*, 1999, **59**, 7413–7421.
4 I. N. Ogorodnikov, V. I. Kirpa and A. V. Kruzhalov, *Technical Physics*, 1993, **38**, 404–408.
5 J. Ghose and A. Roy, Proceedings of the conference of the American Physical Society topical group on shock compression of condensed matter. AIP Conference Proceedings, 1996, pp. 901–904.
6 S. Mochizuki and T. Sakurai, *Physica Status Solidi a-Applied Research*, 1977, **41**, 411–415.
7 M. S. Seehra and H. Wijn, *Magnetic Properties - Magnetic Properties of Non-Metallic Inorganic Compounds Based on Transition Elements - Various Other Oxides - 6.1.5 Oxides of 4d and 5d Transition Elements.*, Springer Materials - The Landolt-Börnstein Database, 1992, vol. 27G.
8 N. N. Kovalev, Y. A. Logachev, A. V. Petrov and O. V. Sorokin, *Sov Phys Solid State*, 1975, **16**, 2367–2368.
9 J. Zhensheng, X. Chanjuan, Z. Qingmei, Y. Feng, Z. Jiazheng and X. Jinzhen, *Journal of Molecular Catalysis - A - Chemical*, 2003, **191**, 61–66.
10 S. Nikitine, *Journal of Physics and Chemistry of Solids*, 1961, **17**, 292–300.
11 L. Tjeng, M. Meinders, van Elp J, J. Ghijsen, G. Sawatzky and R. Johnson, *Physical Review B*, 1990, **41**, 3190–3199.
12 A. M. Herrero, B. P. Gila, C. R. Abernathy, S. J. Pearton, V. Craciun, K. Siebein and F. Ren, *Applied Physics Letters*, 2006, **89**, 2117.
13 J. M. Calleja and M. Cardona, *Physical Review B (Solid State)*, 1977, **16**, 3753–3761.
14 J. Pascual, J. Camassel and H. Mathieu, *Physical Review B (Condensed Matter)*, 1978, **18**, 5606–5614.
15 I. D. Makuta, S. K. Poznyak and A. I. Kulak, *Solid State Communications*, 1990, **76**, 65–68.
16 G. J. B, *Advances in Chemistry CY -*, American Chemical Society, 2011, pp. 113–137.
17 L. Y. L. Shen, G. A. Pasteur and D. E. Aspnes, *Physical Review B (Solid State)*, 1977, **16**, 3742–3745.
18 R. French, S. Glass, F. Ohuchi, Y. Xu and W. Ching, *Physical Review B*, 1994, **49**, 5133–5142.
19 L. Binet, D. Gourier and C. Minot, *Journal of Solid State Chemistry*, 1994, **113**, 420–433.
20 D.-Y. Kim, C.-H. Lee and S. J. Park, *Journal of Materials Research*, 1996, **11**, 2583–2587.
21 R. L. Weiher and R. P. Ley, *Journal of Applied Physics*, 1966, **37**, 299–302.
22 J. M. Themlin, R. Sporken, J. Darville, R. Caudano, J. M. Gilles and R. L. Johnson, *Physical Review B (Condensed Matter)*, 1990, **42**, 71956–11925.
23 V. A. Izvozchikov, *Soviet Physics-Solid State*, 1963, **4**, 2014–2017.
24 E. Salje, *Journal of Applied Crystallography*, 1974, **7**, 615–617.
25 V. Dolocan, *Applied Physics*, 1978, **16**, 405–407.
26 O. Gritsenko, R. van Leeuwen, E. van Lenthe and E. J. Baerends, *Physical Review A (Atomic*, 1995, **51**, 1944.
27 M. Kuisma, J. Ojanen, J. Enkovaara and T. T. Rantala, *Physical Review B*, 2010, **82**, 115106.
28 *ICSD Web*, `http://www.fiz-karlsruhe.de/icsd_web.html`.
29 H. Kato, H. Kobayashi and A. Kudo, *The Journal of Physical Chemistry B*, 2002, **106**, 12441–12447.

30 H. Mizoguchi, H. W. Eng and P. M. Woodward, *Inorg. Chem*, 2004, **43**, 1667–1680.

31 M. A. Butler and D. S. Ginley, *Journal of The Electrochemical Society*, 1978, **125**, 228–232.

32 D. Yamasita, T. Takata, M. Hara, J. Kondo and K. Domen, *Solid State Ionics*, 2004, **172**, 591–595.

33 H. Zhang, Y. Li, Q. Zhang and H. Wang, *Materials Letters*, 2008, **62**, 2729–2732.